Hydrocracking of N-Decane over Zeolite-Supported Metal Sulfide Catalysts. 1. CaY-Supported Transition Metal Sulfides

ARTICLE *in* INDUSTRIAL & ENGINEERING CHEMISTRY RESEARCH · APRIL 1995

Impact Factor: 2.59 · DOI: 10.1021/ie00043a018

5 AUTHORS, INCLUDING:

Henny Zandbergen
Delft University of Technology
668 PUBLICATIONS **18,423** CITATIONS

SEE PROFILE

Hydrocracking of *n*-Decane over Zeolite-Supported Metal Sulfide Catalysts. 1. CaY-Supported Transition Metal Sulfides

Wim J. J. Welters, Onno H. van der Waerden, Henny W. Zandbergen,† Vincent H. J. de Beer,* and Rutger A. van Santen

Schuit Institute of Catalysis, Eindhoven University of Technology, P.O. Box 513, 5600 MB Eindhoven, The Netherlands

The hydrocracking properties of various CaY-supported metal (Fe, Co, Ni, Mo, Ru, Rh, Pd, W, Re, Ir, and Pt) sulfide catalysts (prepared by impregnation) are examined by studying the hydroconversion of *n*-decane. All catalysts show cracking conversions which are significantly higher than that of the CaY support. There are large differences in catalytic behavior dependent on the metal sulfide present on the zeolite support. The amounts of S present on the catalyst are analyzed to determine the degree of sulfidation of the metal sulfide, while high resolution electron microscopy is used to characterize the distribution of the metal sulfide phase over the zeolite support. The observed differences in activity can be explained by the differences in intrinsic activity of the metal sulfide phase and the differences in distribution of this phase over the zeolite particle (internal or external sulfide deposition).

Introduction

Hydrocracking is a typical example of bifunctional catalysis, in which both the hydrogenation/dehydrogenation and the cracking function play a crucial role. Weitkamp *et al.* (Schulz and Weitkamp, 1972; Weitkamp, 1982) and Jacobs *et al.* (Martens *et al.*, 1986a,b; Jacobs and Martens, 1991) have extensively studied the hydrocracking reaction to unravel the mechanism, in particular for the hydrocracking of higher paraffins over noble metal on zeolite catalysts. The reaction starts with the dehydrogenation of the paraffins over the metallic (or metal sulfide) function producing olefins. These form carbenium ions at the acid sites and then undergo the usual acid-catalyzed reactions. At first they are isomerized, that is, if the reaction conditions are severe enough (at prolonged reaction times or higher temperatures), followed by cracking. The products can desorb from the acid sites and be hydrogenated to the corresponding paraffins. If the hydrogenation function is really strong, one usually finds that a substantial degree of isomerization can be achieved with only a little cracking, and that per cracked parent paraffin two product molecules are formed. This is referred to as "ideal hydrocracking" which means that the consecutive reactions (cracking after isomerization, secondary cracking after primary cracking) play a minor role (Jacobs *et al.*, 1980).

Nowadays, hydrocracking catalysts are required to have a flexible product selectivity combined with a high activity. Additionally, they have to be resistant to poisoning by S- and N-containing compounds which are present in feedstocks treated in modern hydrocracking units. This can be achieved by combining a zeolite with a sulfidic hydrogenation function. Transition metal sulfides are effective hydrogenation catalysts and meet the requirements for a high resistance to poisoning by S- and N-containing compounds.

Industrial catalysts mostly use combinations of Mo or W with Ni or Co as the active metal sulfide component (Ward, 1993), and, consequently most of the papers dealing with zeolite-supported transition metal sulfides are focused on these metals (Brooks, 1980; Cid *et al.*, 1985, 1990; Davidova *et al.*, 1986; Kovacheva *et al.*, 1991; Laniecki and Zmierczak, 1991). However, only a few of them include testing of the hydrocracking properties (Langois *et al.*, 1966; Ward, 1983; Yan, 1985; Leglise *et al.*, 1988, 1991b; Esener and Maxwell, 1989). Leglise *et al.* (1988, 1991b) measured the hydrogenation of benzene and the hydrocracking of *n*-heptane over a series of stabilized HY-supported Ni, Mo, and NiMo sulfide catalysts. They found for all these catalysts the hydrogenation function to be considerably weaker than the one found for example in Pt/HY hydroisomerization catalysts (Martens *et al.*, 1986a,b), thus causing a hydrocracking behavior which is far from ideal. Other studies (Ward, 1983; Yan, 1985; Esener and Maxwell, 1989) are much more focused on the optimization of the industrial hydrocracking catalyst and the process conditions than on the fundamental aspects of preparation, structure, and catalytic properties of zeolite-supported transition metal sulfide catalysts.

Besides Co, Ni, Mo, and W there are however many other transition metal sulfides which are comparably or even more active for a range of catalytic reactions, such as thiophene or dibenzothiophene hydrodesulfurization (HDS) (Pecoraro and Chianelli, 1981; Vissers *et al.*, 1984; Ledoux *et al.*, 1986; Lacroix *et al.*, 1989), hydrodenitrogenation (HDN) (Eijsbouts *et al.*, 1988, 1991a,b), or hydrogenation of biphenyl (Lacroix *et al.*, 1989). Combination of an acidic zeolite with these metal sulfides may result in highly active hydrocracking catalysts.

In the present study the hydrocracking properties of several CaY-supported transition metal sulfides are examined by studying the hydroconversion of *n*-decane at moderate pressure (3 MPa). The differences in catalytic activity measured for the various metal sulfides are compared with the trends in activity observed for the above-mentioned test reactions (Pecoraro and Chianelli, 1981; Vissers *et al.*, 1984; Ledoux *et al.*, 1986; Eijsbouts *et al.*, 1988, 1991a,b; Lacroix *et al.*, 1989). In order to allow a meaningful comparison of the catalytic properties between the different metal sulfides, the composition of the metal sulfide phase present on the catalysts is examined by overall sulfur analysis, while

* To whom correspondence should be addressed.

† Centre for High Resolution Electron Microscopy, Delft University of Technology, Rotterdamseweg 137, 2628 AL Delft, The Netherlands.

0888-5885/95/2634-1156$09.00/0

Table 1. CaY-Supported Transition Metal Catalysts Prepared by Impregnation

catalyst	precursor metal salt	metal content[a] (wt %)
Fe/CaY	$FeCl_3 \cdot 6H_2O$ (Merck, >99%)	3.9
Co/CaY	$CoCl_2 \cdot 6H_2O$ (Merck, >99%)	4.1
Ni/CaY	$NiCl_2 \cdot 6H_2O$ (Merck, >99%)	4.1
Mo/CaY	$(NH_4)_6Mo_7O_{24} \cdot 4H_2O$ (Merck, >99%)	6.5
Ru/CaY	$(NH_3)_6RuCl_3$ (Johnson Matthey, 32.6 wt % Ru)	7.0
Rh/CaY	$RhCl_3 \cdot xH_2O$ (Johnson Matthey, 42 wt % Rh)	6.8
Pd/CaY	$Pd(NO_3)_2 \cdot 2H_2O$ (Fluka, >99%)	7.8
W/CaY	$(NH_4)_2W_4O_{13} \cdot 8H_2O$ (Koch-Light Lab., >99%)	11.7
Re/CaY	NH_4ReO_4 (Merck, >99%)	11.9
Ir/CaY	$(NH_4)_3IrCl_6$ (Johnson Matthey, 47 wt % Ir)	14.5
Pt/CaY	$(NH_4)_2PtCl_4$ (Johnson Matthey, 51.5 wt % Pt)	13.9

[a] 100 × weight Me/weight (MeO_x + CaY) with MeO_x respectively Fe_2O_3, Co_3O_4, NiO, MoO_3, RuO_2, Rh_2O_3, PdO, WO_3, Re_2O_7, IrO_2, PtO.

the distribution of the sulfide phase over the zeolite particles on some of the catalysts is characterized by high resolution electron microscopy (HREM). In spite of the fact that stabilized Y zeolites are most commonly used for industrial hydrocracking (Ward, 1983), the original Y zeolite is used as support for our model catalysts in order to avoid changes in catalytic properties or degree of sulfidation of the metal sulfide phase caused by the extraframework alumina or by the presence of mesopores on the stabilized Y zeolite (Leglise *et al.*, 1988).

Experimental Section

Catalyst Preparation. The CaY support ($Ca_{24}Na_6(AlO_2)_{54}(SiO_2)_{138} \cdot xH_2O$) is prepared from a NaY ($Na_{54}(AlO_2)_{54}(SiO_2)_{138} \cdot xH_2O$, PQ CBV-100) zeolite by ion exchange with aqueous $CaCl_2$ solutions followed by washing until Cl^- free. All CaY-supported catalysts are prepared by pore volume impregnation. The concentration of the metal salt is adjusted in order to obtain equal metal loading on a molar basis for all catalysts (0.75 mmol of metal/g of catalyst). After impregnation, the catalyst is dried in static air at 393 K for 16 h, followed by calcination at 673 K for 2 h. The salts used for impregnation and the metal loading in weight percentage are given in Table 1 for each catalyst. All catalysts are stored above saturated $CaCl_2$ solutions. Prior to catalytic testing the powders are pressed, grinded, and sieved to obtain a particle size fraction between 125 and 425 μm.

Hydrocracking of *n*-Decane. All hydrocracking experiments are performed in a microflow reactor containing 0.8 g of dry catalyst mixed with 5 g of SiC (particle size 0.5 mm) at a total pressure of 3.0 MPa. Prior to reaction the catalysts are sulfided *in situ* (6 K min^{-1} from room temperature to 673 K, 2 h at 673 K) in a 10% H_2S in H_2 mixture at 3.0 MPa pressure with a total flow of 100 std cm^3 min^{-1}.

During reaction a H_2S/H_2 gas flow is led over the catalysts (total flow 1250 std cm^3 min^{-1}, $H_2S:H_2$ = 1:1250). H_2S is added to the H_2 feed in order to prevent reduction of the metal sulfides during the hydrocracking test. Liquid *n*-decane is pumped into the system, where it is immediately evaporated and mixed with the H_2S/H_2 gas flow (liquid flow rate of 50 μL min^{-1}, molar ratio *n*-decane:H_2 = 1:200; W/F = 0.37 $g_{cat.}$ h $g_{n\text{-decane}}^{-1}$). Gas samples are taken at the reactor exit and analyzed with an on-line gas chromatograph (GC) equipped with a UCON LB 550 X capillary column. The products with one or two carbon atoms cannot be separated by this analysis, and for the comparison of product selectivities they are therefore denoted as C1−C2. Before starting the activity measurement cycle, the catalyst is stabilized at 673 K for roughly 48 h. Subsequently, the reaction temperature is decreased in steps of approximately 20 K, holding the temperature at each step until the conversion is constant. In this way the *n*-decane conversion is measured as a function of temperature. At the end of each run the temperature was increased to 673 K to examine the deactivation of the catalyst during the entire activity test. For all catalysts this deactivation is less than 3 conversion %.

Catalyst Characterization. Thermogravimetric analysis (TGA) is used to determine the coke content of the deactivated catalysts (oxidation in a 20% O_2/He, Seteram TG 85 balance). Because the oxidation of the coke deposits and the metal sulfide phase cannot be separated, the measured weight loss is corrected for the weight loss due to the oxidation of the metal sulfides to the corresponding metal oxides, assuming the composition of the metal sulfides as determined by overall sulfur analysis.

For the determination of the amount of sulfur present on the catalysts, sulfided samples are dissolved in aqua regia while the mixture is carefully heated. It is experimentally verified that during dissolution no H_2S is formed. During this process the sulfide is converted into sulfate. The amount of sulfate is determined by titration with barium perchlorate. As Ca^{2+} ions disturb the titration, they are removed from the solution by an ion exchanger before titration. The sulfide phases of W, Ru, Rh, and Ir do not dissolve in aqua regia, so another dissolution method had to be used. The tungsten sulfide is fused with NaOH at 725 K; the other sulfides are fused with excess Na_2O_2 at 775 K. The resulting melt is dissolved in water to determine the sulfate content. Before sulfur analysis, the catalysts are sulfided under conditions comparable to reaction conditions: (I) heated in a 10% H_2S in H_2 flow (100 std cm^3 min^{-1}) at 673 K (6 K min^{-1} to 673 K, 2 h at 673 K) and 3.0 MPa, (II) kept under a H_2S/H_2 flow with a ratio of 1:1250 at 673 K and 30 bar for 24 h, (III) flushed with He at 673 K and atmospheric pressure for 1 h, and (IV) cooled to room temperature in a He flow. At room temperature the samples are exposed to air and the analysis procedure is started.

In order to study the distribution of the metal sulfide phase over the zeolite support, high resolution electron microscopy (HREM) experiments are carried out on several sulfided catalysts (sulfidation conditions are the same as for the overall sulfur analysis), using a Philips CM 30 ST electron microscope. The samples are prepared as follows: after grinding, the zeolite particles are suspended in alcohol and a few droplets of the suspension are placed on a copper grid coated with a microgrid carbon polymer. Together with the HREM analysis the transition metal distribution throughout the catalyst particles is determined (integrally or segmentwise) by means of energy dispersive X-ray (EDX) analysis.

Results

***n*-Decane Hydrocracking.** The hydrocracking activity of several CaY-supported transition metal sulfides

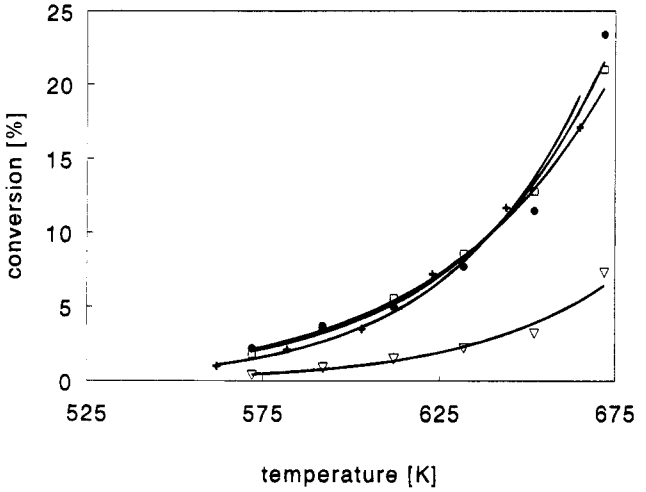

Figure 1. Conversion of *n*-decane as a function of reaction temperature: (▽) CaY; (+) Fe/CaY; (●) Co/CaY; (□) Ni/CaY.

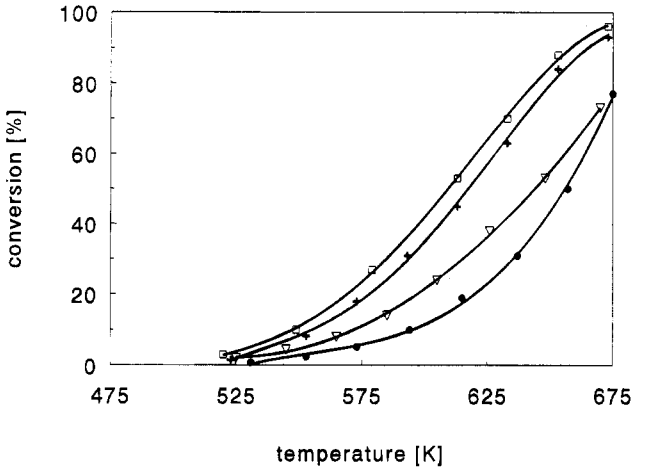

Figure 2. Conversion of *n*-decane as a function of reaction temperature: (+) Mo/CaY; (●) Ru/CaY; (□) Rh/CaY; (▽) Pd/CaY.

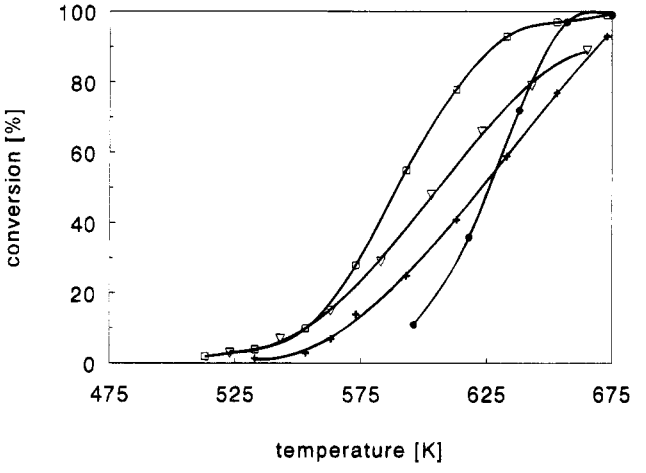

Figure 3. Conversion of *n*-decane as a function of reaction temperature: (+) W/CaY; (●) Re/CaY; (□) Ir/CaY; (▽) Pt/CaY.

is determined. For all catalysts the metal loading is about 0.75 mmol/g CaY, meaning that in the case of ideal metal sulfide dispersion every supercage contains approximately one metal ion. The conversion plotted as a function of reaction temperature of the various catalysts is presented in Figures 1–3. In Figure 1 the conversions measured for Fe, Co, and Ni sulfides are given. All three metal sulfide catalysts show almost equal *n*-decane conversions, which are about 3 times

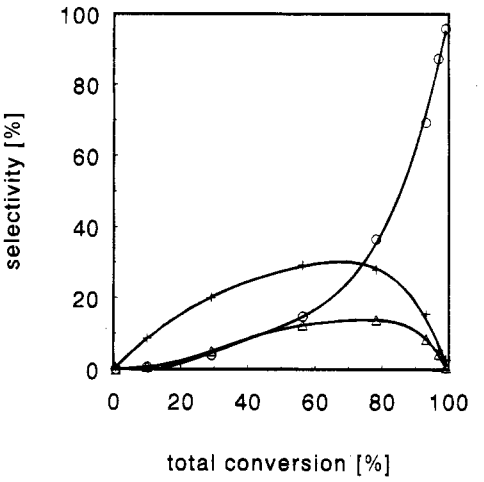

Figure 4. Product selectivities as a function of total conversion as measured for Ir/CaY: (+) monobranched products; (▽) di- or multibranched products; (○) cracked products.

higher than for the pure CaY support. None of the catalysts show any *n*-decane isomerization. The *n*-decane conversion observed for CaY is caused by catalytic cracking over its acid sites and remains low for the reaction temperatures applied in this study. High conversions due to catalytic cracking can only be obtained at temperatures above 673 K.

The activities of Mo, Ru, Rh, and Pd sulfides are given in Figure 2. These catalysts are clearly more active than those shown in Figure 1, and the same applies for W, Re, Ir, and Pt sulfides plotted in Figure 3. It appears that the Mo, W, Pt, and Rh catalysts show comparable conversions as a function of temperature. The Pd and Ru catalysts are slightly less active. At high temperatures (625–675 K) the conversion measured for the Re catalyst is comparable with that of Mo and W catalysts, but its decrease with decreasing temperature is much stronger. At temperatures below 600 K the activity becomes unstable (it varies between 30 and 0%). Clearly, Ir/CaY is the most active catalyst.

Only a few of the above CaY-supported metal sulfide catalysts show feed isomerization. Maximum *n*-decane isomerization selectivities as high as 38 and 32% are measured for Ir/CaY and Rh/CaY, respectively. Of all the other catalysts, Pt/CaY and Pd/CaY have the highest *n*-decane isomerization with maxima of 2.0 and 1.6%, respectively. The isomerization of *n*-decane on the Ir and Rh catalysts resembles the ideal hydrocracking behavior as observed for instance in the case of metallic Pt/CaY catalysts (Weitkamp, 1973), but the positions of the isomerization maxima are shifted toward higher temperatures (about 80–100 K) and their maximum product selectivities for isomerization are lower than for metallic Pt/CaY. In Figure 4 the formation of mono- and multibranched decane isomers as well as cracked products is given as a function of conversion as measured for Ir/CaY. From this figure it becomes clear that the monobranched decanes are the primary products, while only at increasing conversion multibranched decane molecules are formed. Cracking becomes important at even higher total conversions. Rh/CaY shows the same features. The yield pattern shown in Figure 4 is similar to that observed for ideal hydrocracking (Steyns *et al.*, 1981) which indicates that the reaction proceeds via isomerization, first to monobranched decane and in a second step to dibranched or higher branched products, while together with the formation of multibranched decane molecules also cracking occurs.

Table 2. Product Distributions Expressed as Moles of C*x* Product per Mole of Converted *n*-Decane

catalyst	conv (reaction temp (K))	total production C*x*,[a] 100 × (mol of C*x*/mol of converted C10)							
		C1/C2	C3	C4	C5	C6	C7	iC10	NC*x*/NC10[b]
CaY	7% (673)	11.4	49.5	76.5	56.4	39.1	4.2	0	2.37
Fe/CaY	12% (644)	3.0	29.2	64.7	56.7	45.2	8.6	3.3	2.15
Co/CaY	10% (652)	7.4	31.4	64.3	56.9	44.4	8.0	3.4	2.20
Ni/CaY	13% (654)	7.1	37.9	70.5	58.3	43.8	6.2	0	2.24
Mo/CaY	13% (569)	3.9	21.3	64.1	60.9	46.9	9.3	2.5	2.12
Ru/CaY	10% (594)	0	25.4	65.9	59.2	47.0	9.7	1.4	2.10
Rh/CaY	27% (579)	0	2.9	9.2	10.9	9.0	2.3	83.0	2.02
Pd/CaY	16% (585)	0	17.5	57.0	59.3	49.0	9.5	6.0	2.05
W/CaY	14% (572)	0	20.0	62.4	60.8	49.0	10.0	2.2	2.07
Re/CaY	11% (597)	5.7	16.6	51.1	55.9	49.0	11.7	8.5	2.08
Ir/CaY	28% (571)	0	2.2	7.7	9.2	7.6	1.8	85.8	2.01
Pt/CaY	15% (563)	0	14.6	54.4	57.5	49.5	10.6	8.2	2.04
Mo/CaY	90% (673)	7.5	48.4	81.6	58.8	35.2	2.3	0	2.33
Rh/CaY	95% (672)	9.0	16.7	47.4	51.7	45.3	11.8	13.9	2.11
W/CaY	93% (672)	6.6	47.5	81.8	59.1	35.3	2.3	0	2.32
Re/CaY	99% (675)	10.4	35.9	68.8	59.9	47.7	4.0	0	2.26
Ir/CaY	99% (673)	2.5	17.9	53.3	58.3	51.4	13.5	3.3	2.04
Pt/CaY	89% (670)	1.3	33.1	65.1	59.4	47.7	5.1	2.0	2.16

[a] The formation of C8 and C9 has not been observed. [b] Mole cracking products (NC*x*) per mole of *n*-decane cracked (NC10).

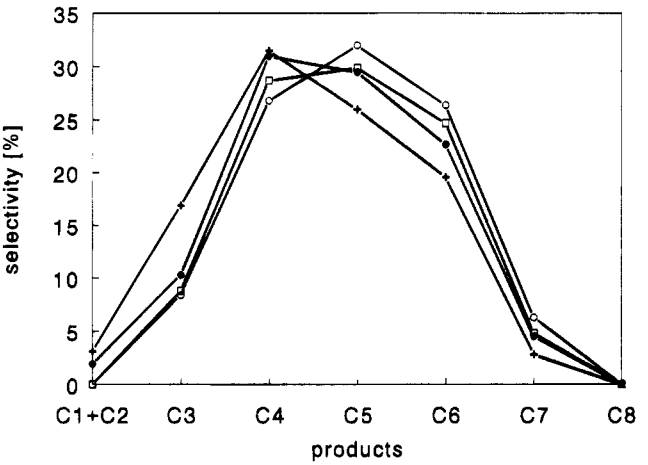

Figure 5. Product selectivities as a function of molecule size (C*x*) for different catalysts: (○) Ir/CaY; (□) Pd/CaY; (●) Mo/CaY; (+) Ni/CaY.

The presence of the branched decane products indicates that the olefins which desorb from the acid site are hydrogenated quickly to the corresponding paraffins. Apparently, the CaY-supported Rh and Ir sulfide catalysts have a strong (de)hydrogenation function.

All other catalysts show hardly any *n*-decane isomerization, in spite of the fact that some of them (Mo, W, Re, Pt) show high conversions for *n*-decane cracking, comparable with that of the Rh/CaY catalyst. The hydrogenation function of the sulfide phase present in these catalysts is too weak to hydrogenate the olefins which desorb from the acid sites before they are adsorbed again and cracked. Evidently, the (de)hydrogenation function of all these catalysts is considerably less strong than that of the Rh and Ir sulfide catalysts.

On the basis of the performed hydrocracking tests, it is difficult to give an accurate comparison of the product selectivities for the various hydrocracking catalysts included in this study. In case cracking is ideal, the product selectivity is only dependent on the conversion (Steijns *et al.*, 1981) and a comparison of the catalyst product selectivities can be made at one conversion level, independent of the reaction temperature. When secondary cracking occurs, the product selectivity becomes a function of both the conversion level and the reaction temperature (or the space velocity). In this case an extensive comparison of the various catalyst product selectivities cannot be made since they are depending not only on the type of metal sulfide but also on the reaction conditions. Nevertheless, a careful examination of the observed product selectivities can still give valuable information. In Table 2 the product selectivities of the CaY-supported metal sulfide catalysts are given as a function of the number of carbon atoms in the product molecules for two different conversion levels. Since the amounts of alkenes usually remained below the detection limit, only alkane-type products are given in Table 2.

The Ir and Rh sulfide catalysts show a symmetric pattern in their product distribution as can be seen in Figure 5 for Ir/CaY, indicating that only primary cracking occurred. Also the number of product molecules per cracked *n*-decane molecule at low conversions (last column in Table 2) shows that hardly any secondary cracking occurs on these catalysts. At high conversions the degree of secondary cracking is of course somewhat higher. The other catalysts do not show a symmetric product distribution at low conversions, which implies the presence of secondary cracking (see Table 2 and Figure 5). Also from the number of product molecules per cracked *n*-C10 molecule it can be concluded that the degree of secondary cracking is higher on the other catalysts, varying from slightly higher for the Pt, Pd, and W sulfide catalysts to very high for the Co and Ni sulfide catalysts. However, as these product selectivities are compared at equal conversion and not at the same reaction temperature, the high degree of secondary cracking, especially for the Ni and Co catalysts, can partly be due to the high reaction temperatures needed to obtain the conversion at which the comparison is made. On the other hand, when the secondary cracking activity of Ni and Co catalysts at 654 K is compared with that of Ir and Rh catalysts at 673 K (at a conversion of almost 100%), we can see that they still show a far higher degree of secondary cracking. Obviously the differences in secondary cracking between the different metal sulfide catalysts are to a large extent caused by the variations in hydrogenation strength between the various catalysts. For catalysts with a weak hydrogenation function the product olefins are cracked again before they can be hydrogenated, resulting in a high degree of secondary cracking. From the conversions and the product distributions we can roughly rank the CaY-supported metal sulfide catalysts

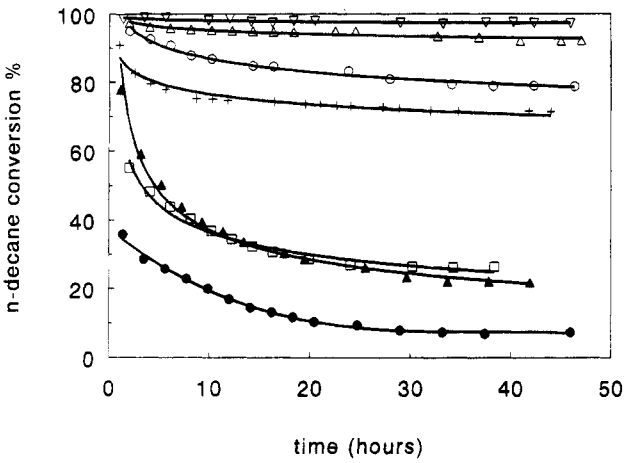

Figure 6. Deactivation as a function of run time: (+) Pd/CaY; (△) Mo/CaY; (○) Ru/CaY; (▽) Rh/CaY; (□) Co/CaY; (▲) Ni/CaY; (●) CaY.

Table 3. Coke Contents of the Deactivated CaY-Supported Metal Sulfide Catalysts

catalyst	amt of coke (wt %)	catalyst	amt of coke (wt %)
CaY	20.1	Rh/CaY	5.4
Fe/CaY	10.7	Pd/CaY	3.2
Co/CaY	13.4	W/CaY	13.8
Ni/CaY	15.8	Re/CaY	8.9
Mo/CaY	15.4	Ir/CaY	4.4
Ru/CaY	12.0	Pt/CaY	1.5

in order of decreasing (de)hydrogenation strength: Ir > Rh > Pt, Pd, Mo, Re, W > Ru > Fe, Ni, Co.

Prior to the conversion measurements the catalysts are stabilized during 48 h. During this period large differences in deactivation behavior are observed (Figure 6). Whereas some catalysts like Ni/CaY, Co/CaY, Fe/CaY (not shown), and CaY deactivate considerably, others deactivate less (Ru/CaY, Pd/CaY, and Pt/CaY (not shown)) or not at all (Mo/CaY, Rh/CaY, Ir/CaY (not shown), and Re/CaY (not shown)). After 48 h some of the catalysts still show a very slow deactivation. However, the influence of this slow deactivation on the conversion levels appears to be negligible.

In Table 3 the results of coke analysis are presented. As was to be expected, all CaY-supported metal sulfides contain less coke than the pure CaY zeolite. The coke content of Rh/CaY and Ir/CaY is very low. This is in line with the earlier conclusion that they show almost ideal hydrocracking behavior, and thus probably have a strong hydrogenation function. Pd/CaY and Pt/CaY contain even smaller amounts of coke in spite of the fact that their hydrogenation function is less strong. All other catalysts have considerably higher coke contents. The deactivation observed for some catalysts can be explained by this coking. Probably coke is covering acid sites during the first hours of reaction, causing a decrease in activity. Mo/CaY and W/CaY catalysts contain a very large amount of coke in spite of their high catalytic activity. Possibly, on these catalysts the coke does not cover sites that contribute significantly to the conversion.

Overall Sulfur Analysis. One reason for the surprisingly high hydrogenation properties of the Ir and Rh catalysts might be that these catalysts are not fully sulfided under reaction conditions. The low H_2S/H_2 ratio might cause a partial reduction of the Rh or Ir sulfide phase during reaction conditions. Mangnus (1991) showed that the metal sulfide phase present in the catalyst can be strongly dependent on the H_2S/H_2 ratio. Also the support can have an influence on the metal sulfide phase (Burch and Collins, 1986).

Table 4. Degree of Sulfidation of the CaY-Supported Metal Sulfide Catalysts[a]

catalyst	metal content (wt %)	Me:S ratio	metal sulfide phase[b]
Fe/CaY	3.9	1:1.0	FeS
Co/CaY	4.1	9:8.2	Co_9S_8
Ni/CaY	4.1	3:2.1	Ni_3S_2
Mo/CaY	6.5	1:1.6	MoS_2
Ru/CaY	7.1	1:1.2	RuS_x
Rh/CaY	6.9	2:3.2	Rh_2S_3
Pd/CaY	7.8	1:1.0	PdS
W/CaY	11.7	1:2.2	WS_2
Re/CaY	11.8	1:2.2	ReS_2
Ir/CaY	14.7	1:1.2	IrS_x
Pt/CaY	13.9	1.1.0	PtS

[a] Sulfidation procedure: (I) heating in a 10% H_2S in H_2 flow (100 std cm^3 min^{-1}) at 673 K (6 K min^{-1} to 673 K, 2 h at 673 K) and 3.0 MPa, (II) isothermal stage in a H_2S/H_2 flow with a ratio of 1:1250 at 673 K and 30 bar for 24 h, (III) flushing with He at 673 K and atmospheric pressure for 1 h, and (IV) cooling down to room temperature in a He flow. [b] Metal sulfide expected after sulfidation on the basis of thermodynamics (Mangnus, 1991).

To verify their degree of sulfidation, the catalysts are sulfided under conditions comparable to reaction conditions (first sulfidation in 10% H_2S/H_2 at 673 K, followed by 24 h equilibration at a H_2S/H_2 ratio of 1:1250 at 3.0 MPa), and the sulfur content is subsequently analyzed. From the Me/S ratios given in Table 4 it can be concluded that after the sulfidation procedure the Ni, Co, Fe, Pd, W, and Re catalysts contain the metal sulfide phase which is to be expected on the basis of thermodynamics (Mangnus, 1991). In the case of Mo/CaY, not all Mo has been converted into MoS_2, which is the thermodynamically stable phase under "reaction" conditions (H_2S/H_2 ratio of 1:1250). The incomplete sulfidation is most likely due to the formation of Mo species which are difficult to sulfide, such as large MoO_3 crystals on the exterior of the zeolite particles (Welters *et al.*, 1994a). For Ru/CaY, Rh/CaY, Ir/CaY, and Pt/CaY the Me:S ratio differs from the one predicted by thermodynamics (Mangnus, 1991). Under "reaction" conditions Rh_9S_8 and platinum metal are predicted to be the most stable phases for Rh/CaY and Pt/CaY, respectively. Nevertheless Rh_2S_3 and PtS are found to be present in these catalysts. Possibly, these sulfides are formed during sulfidation (H_2S/H_2 = 1:10) prior to equilibration (H_2S/H_2 = 1:1250).

For Ru/CaY and Ir/CaY the Me:S ratio does not correspond to a known metal sulfide phase (Vissers *et al.*, 1984; Lacroix *et al.*, 1989; Mangnus, 1991). From the available thermodynamical data it is not possible to decide which sulfide will be present under "reaction" conditions.

The Re/CaY catalyst appears to give a different metal sulfide phase when it is kept under reaction conditions (3.0 MPa, H_2S/H_2 = 1:1250) at a temperature of 553 K instead of 673 K. Overall sulfur analysis revealed that the rhenium sulfide phase of a Re/CaY catalyst kept at 553 K for 24 h has a Re:S ratio of 1:2.9. This can be explained by assuming that ReS_2 formed during the *in situ* sulfidation pretreatment (10% H_2S/H_2, 673 K) is slowly converted into Re_2S_7. Due to the low temperature the conversion will be very slow and still not completed after 24 h, resulting in a sulfur content in between that of ReS_2 and Re_2S_7. Also Ledoux *et al.* (Ledoux *et al.*, 1986) found a phase transition for the rhenium sulfide catalyst at almost the same temperature.

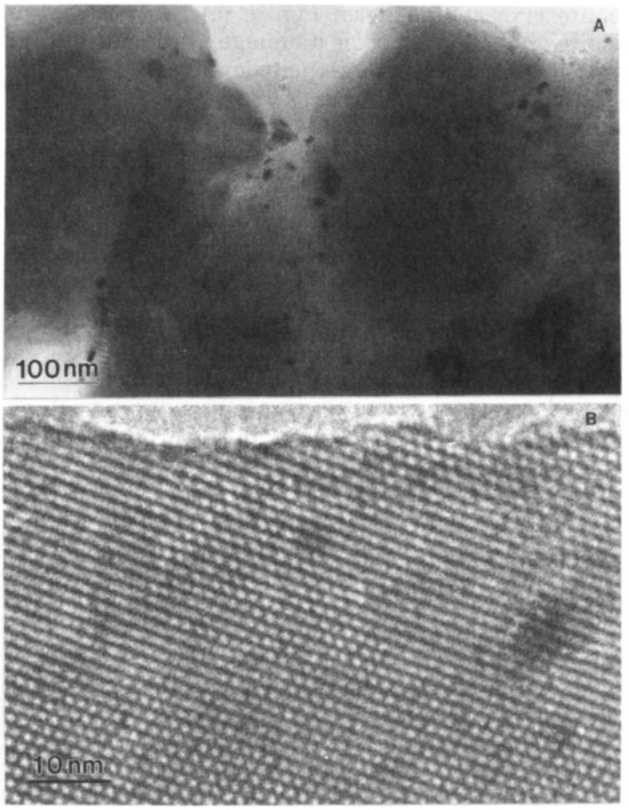

Figure 7. HREM pictures of sulfided Co/CaY.

Generally, the metal sulfide phases (except for Mo/CaY) correspond well with those found by X-ray photoelectron spectroscopy in carbon-supported metal sulfide catalysts as reported by Vissers *et al.* (1984). Also for the unsupported metal sulfide catalysts the same sulfides are found at similar conditions (first presulfidation at 673 K in a 15% H_2S/H_2 flow, followed by reaction under 3.1 MPa H_2 pressure) (Pecoraro and Chianelli, 1981), except for Ir/CaY.

Possibly on some catalysts elemental sulfur is present, which would complicate an exact determination of the metal sulfide phase and the degree of sulfidation. However, in the presence of a transition metal sulfide elemental sulfur can be reduced (H_2S formation) at the conditions used for catalyst sulfidation (Arnoldy *et al.*, 1985; Mangnus, 1991). Nevertheless, overall sulfur analysis is not the most preferable method to identify the metal sulfide phase present in this type of (hydrocracking) catalysts since it determines not only sulfide sulfur but also elemental sulfur which can be formed during sulfidation. Therefore, other techniques, such as temperature programmed sulfidation and reduction, have to be used to obtain more precise information on the metal sulfide phase and the presence of elemental sulfur on these hydrocracking catalysts.

HREM and EDX. The distribution of the metal sulfide phase over the zeolite particles can have a strong influence on the hydrocracking properties. In order to see whether there are large differences in the metal sulfide distribution, HREM is performed on some of the sulfided catalysts (sulfidation conditions the same as for sulfur analysis).

For Ni/CaY sulfided at 3.0 MPa (sulfidation conditions the same as for the sulfur analysis) the HREM measurements show that a large fraction of the nickel sulfide is located on the outside of the zeolite particles (pictures not shown). Combination of HREM with EDX experiments can provide additional information on the distribution of the nickel sulfide over the zeolite particles. The average Ni/Si ratio in the EDX spectrum of a great number of zeolite particles is compared with the ratio of a spot on a zeolite particle not containing nickel sulfide at its outer surface. From this comparison an estimation of the relative amounts of nickel sulfide located in the zeolite pore system can be made. The combined HREM–EDX experiments show that approximately 15% of the total amount of Ni is located inside the zeolite pores.

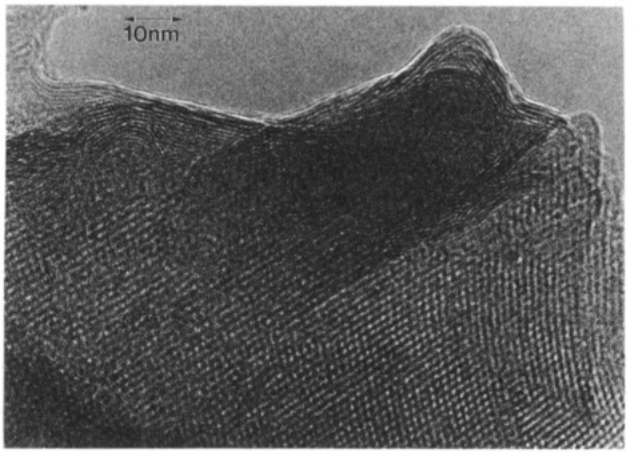

Figure 8. HREM picture of sulfided Mo/CaY.

HREM pictures of a sulfided Co/CaY catalyst (Figure 7A) show the presence of large cobalt sulfide particles (black spots) on the outside of the zeolite particles. The cobalt sulfide particles can be as large as 50 nm, but also very small cobalt sulfide particles (approximately 3 nm) are present. The two dark spots in Figure 7B are most likely cobalt sulfide particles, while the grid is caused by the zeolite framework. These small cobalt sulfide particles might be located inside the zeolite pores, although they are too large to fit into one supercage. The amount of Co located in the zeolite pores can be estimated at about 10% of the total amount of Co present. This implies that most of the cobalt sulfide is located on the outside of the zeolite particles.

Figure 8 shows a HREM picture of a sulfided Mo/CaY catalyst. The large MoS_2 slabs on the outside of the zeolite particles are clearly visible. The zeolite particles are to a large extent covered by the MoS_2 slabs which are sometimes stacked up to 10 or more layers. Clearly, a large fraction of the molybdenum sulfide is located on the outer zeolite surface. From HREM–EDX measurements it is inferred that a relatively small fraction of the molybdenum is located inside the zeolite pores (Welters *et al.*, 1994a). The latter fraction is estimated to correspond to about 15% of the total molybdenum content. Besides the large MoS_2 slabs also some large particles (up to 100 nm) consisting of MoS_2 and some amorphous material can be observed on the outside of the zeolite. The EDX results show that these particles contain Ca atoms. Also on the oxidic samples (before sulfidation) some particles are observed which contain, besides O, mainly Ca and Mo, and hardly any Al or Si. This suggests that a calcium molybdenum oxide (probably $CaMoO_4$) has been formed after impregnation and calcination. Possibly, some of the Ca^{2+} ions of the CaY support are leached out during impregnation (they might have been replaced by the NH_4^+ ions of the $(NH_4)_6Mo_7O_{24}$)), leading to the formation of $CaMoO_4$ on the surface of the zeolite framework. Upon sulfidation the particles containing $CaMoO_4$ are partly converted

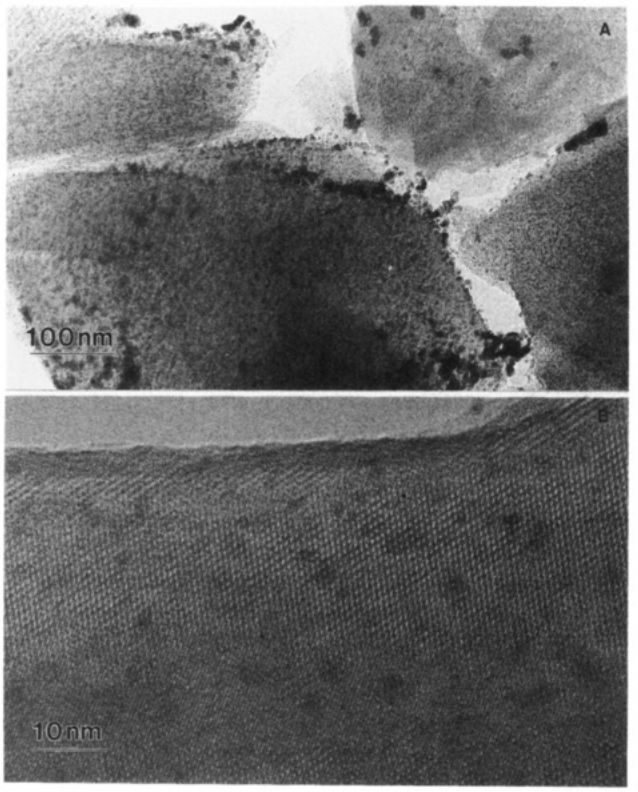

Figure 9. HREM pictures of sulfided Ir/CaY.

into MoS_2. But, as $CaMoO_4$ is probably difficult to sulfide, some $CaMoO_4$ will remain after sulfidation resulting in the presence of large particles consisting of MoS_2 and some amorphous material.

The distribution of the RuS_x over the zeolite particles is again very inhomogeneous (HREM pictures not shown). Some zeolite particles contain almost exclusively very large ruthenium sulfide particles at their outer surface, whereas others contain both large and small ones. The small RuS_x particles are probably located in the zeolite pores. EDX experiments revealed that even for those zeolite particles on which a large number of small sulfide particles are visible only relatively little ruthenium is actually present in the zeolite pores (approximately 15%). Apparently, the larger part of the ruthenium is located on the exterior of the zeolite particles as large sulfide crystals.

Similar to the Ru/CaY, the Rh/CaY catalyst contains large sulfide particles (Rh_2S_3) at the outer zeolite surface (pictures not shown), albeit they are less abundant and there are more small particles present which are probably located inside the zeolite pores. This is corroborated by EDX results on zeolite particles which contain no large rhodium agglomerates on the exterior showing that approximately 40% of the total Rh content is present in the zeolite pores. Probably, the Rh_2S_3 phase is distributed more homogeneously throughout the zeolite particles than for instance the metal sulfide phase on the Mo/CaY, Ni/CaY, or Ru/CaY catalysts.

As can be seen from Figure 9, a sulfided Ir/CaY again contains quite a number of large sulfide particles (IrS_x) inhomogeneously distributed over the outside of the zeolite particles, but it can clearly be seen that in addition to this there are many small dark spots which are homogeneously distributed over the zeolite particle. These dark spots represent small IrS_x particles probably located inside the zeolite pores. The concentration of spots (metal sulfide particles) increases with increasing zeolite crystal thickness (Figure 9A; the thicker the zeolite crystal, the darker its image in the micrograph, and the darker zeolite particles contain a higher density of small iridium particles). This suggests that these particles are located inside the zeolite pores, since otherwise their concentration should be independent of the thickness of the zeolite crystal. The metal sulfide fraction located inside the zeolite pores is comparable to the Rh/CaY catalysts. In Figure 9B a large number (compared to for instance Co/CaY or Ru/CaY) of small metal sulfide particles present inside the zeolite pores can be seen. The size of the iridium particles varies between 1 and 4 nm. As for the Co/CaY and Ru/CaY catalysts, the small IrS_x particles which are probably located inside the zeolite pores are larger than the supercage dimensions, a phenomenon which has also been observed for metallic Pt/CaY zeolites (Lunsford and Treybig, 1981). The explanation can be that the IrS_x cluster occupies several neighboring supercages, or that it is located in voids and defects in the zeolite crystal. These voids may have been formed during the formation of the metal sulfide particles.

A general conclusion which can be drawn from the above results is that on those catalysts which are examined by HREM a large fraction of the metal sulfide phase is located at the outside of the zeolite particles. Still there are some differences between the various metal sulfide catalysts. Compared with the Ni, Co, Mo, or Ru catalysts, on Rh/CaY and Ir/CaY a relatively large part of the sulfide phase is inside the zeolite pores as very small particles. For Co/CaY, Ni/CaY, Mo/CaY, or Ru/CaY the amount of metal sulfide inside the zeolite pores is very small.

Discussion

Most of the CaY-supported metal sulfide catalysts show high conversions for cracking of *n*-decane compared with the pure CaY support, but their catalytic properties are nevertheless far from ideal hydrocracking behavior, as observed for instance on metallic Pt/CaY catalysts (Schulz and Weitkamp, 1972; Jacobs *et al.*, 1980; Weitkamp, 1982). There are large differences in hydrocracking properties between the various metal sulfide catalysts, which correlate roughly with the activity trends observed for other sulfide catalyzed reactions like thiophene HDS (Vissers *et al.*, 1984; Ledoux *et al.*, 1986), HDS of dibenzothiophene at low (Lacroix *et al.*, 1989) or high (Pecoraro and Chianelli, 1981) pressure, HDN of quinoline (Eijsbouts *et al.*, 1988, 1991a,b), and the hydrogenation (HYD) of biphenyl (Lacroix *et al.*, 1989).

Compared with the activity trends for typical HDS, HDN, and HYD reactions, the trend measured for hydrocracking of *n*-decane shows some striking differences. Re and especially Mo and W sulfide catalysts show a surprisingly high hydrocracking activity in comparison with the other metal sulfides like Pd, Pt, Rh, and Ir. The Ru catalyst shows a relatively low *n*-decane conversion, while for all other test reactions the Ru sulfide is one of the most active catalysts. Similar to the trends measured for the other test reactions, the Fe, Co, and Ni sulfide are the least active hydrocracking catalysts, although the difference in activity between these catalysts and the other metal sulfides seems to be large compared to the picture that emerges from relative activities for HDS, HDN, and HYD reactions. A more detailed comparison of the activity trends for distinct test reactions is not possible

due to the differences between the test reactions, the reaction conditions, and the various preparation methods used for the metal sulfide catalysts. Especially for the zeolite-supported metal sulfide catalysts both the position of the metal sulfide (in the zeolite pores or on the exterior) and the dispersion may have a strong influence on the catalytic activity, as will be discussed below.

From the product distributions shown in Table 2 some conclusions can be drawn concerning the cracking mechanisms taking place on the various catalysts. Several catalysts show a considerable production of C1–C2 molecules especially at high reaction temperatures. Since products containing only one or two carbon atoms could not be separately analyzed by the GC system used, they will be treated as a lumped fraction referred to as C1–C2. Their formation cannot be the result of β-scission as, according to the stability rules of the carbenium ion, the formation of C1 and C2 products during this cracking reaction is not favored (Martens *et al.*, 1986a,b; Jacobs and Martens, 1991). The C1–C2 production may be caused by hydrogenolysis (Sinfelt, 1973) or by cracking via a nonclassical pentacoordinated carbonium ion (PCI) as intermediate (Haag and Dessau, 1984; Mirodatos and Barthomeuf, 1988). If hydrogenolysis occurs on these catalysts, it should take place on the metal sulfide phase. The fact that NaY-supported Mo and Ni sulfide catalysts (which show hardly any activity in the hydrocracking reaction due to the absence of acid sites) do not produce C1–C2 is a strong indication that also the corresponding CaY-supported metal sulfide catalysts do not produce C1 and C2 via hydrogenolysis. In addition, the fact that the pure CaY zeolite yields a considerable amount of C1–C2 strongly indicates that C1–C2 formation is not due to hydrogenolysis, but to cracking via the PCI intermediate. For all catalysts, C1–C2 formation increases strongly with increasing reaction temperature. Apparently cracking via the PCI intermediate is mainly dependent on the reaction temperature. The conversion and the hydrogenating properties of the metal sulfide have a small influence on the degree of cracking via the PCI intermediate.

Also secondary cracking does not proceed exclusively via β-scission. If we assume β-scission to be the only secondary cracking reaction, each 2-fold splitted decane molecule is converted into two C3 and one C4 molecules. From Table 2 we can calculate the amounts of secondary cracking products by subtracting the primary cracking products (this means subtracting equal amounts of C3 and C4 as there are C7 and C6 products). These amounts are given in Table 5. For almost all catalysts the C4/C3 ratio is far higher than expected if only secondary cracking is taking place. So, the β-scission mechanism alone cannot explain this product distribution. Also abstraction of C1 or C2 molecules via the PCI cracking mechanism, followed by further cracking via β-scission cannot explain the high C4 production (the C1–C2 production is too low to explain the excess formation of C4 products). Langois et al. (1966) observed the same features on silica–alumina supported nickel sulfide catalysts. A possible explanation can be the occurrence of bimolecular reactions between for instance alkenes and carbenium ions resulting in the formation of heavier carbenium ions:

$$C_nH_{2n} + C_mH_{2m+1}^{+} \rightleftharpoons C_{n+m}H_{2(n+m)+1}^{+} \rightarrow \text{cracking}$$

Leglise *et al.* (1991a) proposed this formation of large carbenium ions in the cracking of *n*-nonane over poorly dispersed Pd/HY catalysts. These carbenium ions will probably almost immediately be cracked into small molecules. As a consequence of this side reaction, the product distribution will be changed. The high reactivity of these large carbenium ions (Weitkamp, 1978; Sie, 1993) is probably the reason why large product molecules are never detected (only occasionally traces of C8 products are found). They are also very likely coke precursors. Also Vasquez *et al.* (1987) observed (C6 + C5 + C4)/(C1 + C2 + C3) ratios higher than 1 in cracking of *n*-heptane over oxidic Ni–Mo/HY zeolites and concluded that consecutive alkylation–cracking reactions occurred.

Table 5. Product Distribution from Secondary Cracking

catalyst	total conv	temp (K)	secondary cracking products, 100 × (mol of Cx/mol of converted C10) C3	C4
Fe/CaY	12%	644	20.6	19.5
Co/CaY	10%	652	23.4	19.9
Ni/CaY	13%	654	31.7	26.7
Mo/CaY	13%	569	12.0	17.2
Ru/CaY	10%	594	15.7	18.9
Rh/CaY	27%	579	0.6	0.2
Pd/CaY	16%	585	8.0	8.0
W/CaY	14%	572	10.0	13.4
Re/CaY	11%	597	4.9	2.1
Ir/CaY	28%	571	0.6	0.1
Pt/CaY	15%	563	4.0	4.9
Mo/CaY	90%	673	46.1	46.4
Rh/CaY	95%	672	4.9	2.1
W/CaY	93%	672	45.2	46.5
Re/CaY	99%	675	31.9	21.1
Ir/CaY	99%	673	4.4	1.9
Pt/CaY	89%	670	28.0	17.4

The almost ideal hydrocracking behavior of the Rh and Ir sulfide catalysts contrasts sharply with the total absence of ideal hydrocracking features on all the other catalysts. The reason for the relatively good hydrocracking properties of these two catalysts is probably not the presence of a metal instead of a sulfide phase (as overall sulfur analysis showed that there are large amounts of sulfur present on these catalysts), but a combination of a relatively good distribution of the metal sulfide phase throughout the pores of the zeolite particle combined with a high intrinsic hydrogenation activity of these metal sulfides, as has already been reported by others (Pecoraro and Chianelli, 1981; Lacroix *et al.*, 1989). This is probably also the reason for the low degree of coke formation found for these catalysts. Also for the Pd/CaY and Pt/CaY the metal sulfide distribution will probably be relatively homogeneous, but as the hydrogenation properties of these metal sulfides are less strong compared to Ir and Rh sulfide, the Pd/CaY and Pt/CaY catalysts show lower conversions and no ideal hydrocracking behavior.

Compared to the other catalysts the Ru catalyst shows a relatively low activity and a high degree of coke formation. This is probably the consequence of a very poor metal sulfide dispersion, as measured by HREM. The reason for the relatively low hydrocracking conversions of the Ni, Co, and Fe catalysts is most likely also the very inhomogeneous distribution of the metal sulfide phase over the zeolite particles. For the Co and Ni catalysts it was shown by HREM that a large part of the sulfide phase is located on the outside of the zeolite crystals as large metal sulfide particles. The relatively small amounts of metal sulfide present in the pores of the zeolite for Ni/CaY and Co/CaY (as observed with the combined HREM–EDX measurements) agree well with

the large coke contents found after reaction. Because there are only small amounts of hydrogenating sulfide species present in the pores, coke formation cannot be prevented and is therefore high.

Also for Mo/CaY and W/CaY much coke is found to be present after reaction. But in spite of the large coke contents and the most probably low dispersion of the metal sulfide, these catalysts show surprisingly high hydrocracking conversions. The product selectivities of these catalysts however show that there is a strong imbalance between the hydrogenation function and the acidic function, resulting in a high degree of secondary cracking.

For the Mo/CaY catalyst it is shown that probably some of the Ca^{2+} ions are leached out of the zeolite support during impregnation (HREM–EDX results). Also for the W/CaY catalysts some removal of Ca^{2+} from the zeolite support may have occurred. This may lead to a stronger acidity of the zeolite support after sulfidation, and consequently to a higher hydrocracking activity. The amount of Ca-containing Mo particles as observed by HREM is low, indicating that the Ca removal will cause only a rather small increase of the acidity of the zeolite support. It is not clear whether this effect is strong enough to explain the relatively high hydrocracking activities of the Mo and W catalysts. It may explain however the very high degree of coking observed on these catalysts.

In agreement with the results reported by Leglise *et al.* (1988) the Mo/CaY is not fully sulfided. The incomplete sulfidation may have been caused by the presence of large molybdenum oxide particles on the exterior of the zeolite particles (Welters *et al.*, 1994a). Furthermore, the $CaMoO_4$ formed after impregnation may be difficult to convert into MoS_2. The HREM results however suggest that the $CaMoO_4$ particles are partially converted into MoS_2. The presence of incompletely sulfided molybdenum oxide or $CaMoO_4$ particles may have some influence on the hydrocracking properties of the Mo/CaY catalyst. But, as most of these particles will be partially or completely covered by MoS_2 layers (the surface of the molybdenum oxide particles is usually more easily sulfided than the core (Arnoldy *et al.*, 1985)), their influence on the catalytic properties will not be very strong.

In view of the incomplete sulfidation of the Mo/CaY catalyst, the full sulfidation of the W/CaY catalyst (measured by overall sulfur analysis) is somewhat surprising. Scheffer *et al.* (Scheffer *et al.*, 1990) showed that both WO_3 and W/Al_2O_3 catalysts are difficult to sulfide. Additionally W/CaY may also contain large bulklike WO_3 particles and/or $CaWO_4$ which, comparable with the Mo/CaY catalyst, should hamper the sulfidation.

Re/CaY also shows a high hydrocracking conversion at high reaction temperatures, but the degree of secondary cracking and the coke formation on this catalyst are lower than on Mo/CaY and W/CaY, indicating a better balance between the hydrogenation and the acidic function on this catalyst. The unstable conversions measured at temperatures below 600 K are most likely caused by the phase transition of the ReS_2 to Re_2S_7 (Ledoux *et al.*, 1986). Because of the low temperatures and the low H_2S/H_2 ratio, the phase transition will be very slow (overall sulfur analysis showed that after 24 h at 550 K this transition is still not completed) which explains why the conversion remains unstable for a long period of time.

Summarizing, it can be concluded that the activity trend for hydrocracking measured for CaY-supported metal sulfides is determined by both the hydrogenation properties of the metal sulfide and its distribution over the zeolite particle. On all catalysts except Rh/CaY and Ir/CaY the hydrogenation function is too weak to obtain ideal hydrocracking behavior. The distribution of the metal sulfide over the zeolite particle is very inhomogeneous for all catalysts (even for Rh/CaY and Ir/CaY only 40% of the metal sulfide is located in the zeolite pores). A large part of the sulfide is located on the outside of the zeolite particles. As a result, the catalysts show a high degree of coke formation and a strong imbalance between the hydrogenation and the acidic function. Possibly, higher conversions and/or catalytic properties closer to ideal hydrocracking could be obtained via preparation methods resulting in a high metal sulfide dispersion and a homogeneous distribution of the metal sulfide throughout the zeolite particles.

Conclusions

All the CaY-supported metal sulfide catalysts show cracking conversions which are significantly higher than that of the CaY support. Their hydrocracking activity is determined by both the hydrogenation properties of the metal sulfide present and its distribution over the zeolite particle. The relatively good distribution of the Rh and Ir sulfide phase throughout the zeolite particle, combined with their intrinsically strong hydrogenation properties (Pecoraro and Chianelli, 1981; Vissers *et al.*, 1984; Ledoux *et al.*, 1986; Eijsbouts *et al.*, 1988, 1991a,b; Lacroix *et al.*, 1989), results in almost ideal hydrocracking behavior for sulfided Rh/CaY and Ir/CaY. Those catalysts having a metal sulfide phase mainly located on the outside of the zeolite crystals show a high degree of coking, lower conversions, and nonideal hydrocracking properties. Mo/CaY and W/CaY show relatively high hydrocracking conversions in spite of the high amount of metal sulfide located on the outside of the zeolite crystals and the high degree of coke formation. This can be due to a relatively high acidity of the zeolite caused by the exchange of Ca^{2+} by NH_4^+ during impregnation.

Acknowledgment

These investigations are supported by the Netherlands Foundation for Chemical Research (SON) with financial aid from the Netherlands Technology Foundation. The HREM measurements are conducted at the Delft University of Technology with the assistance of Mr. C. D. de Haan.

Literature Cited

Arnoldy, P.; van den Heykant, J. A. M.; de Bok, G. D.; Moulijn, J. A. Temperature programmed sulfiding of MoO_3/Al_2O_3 catalysts. *J. Catal.* **1985**, *92*, 35.

Brooks, C. S. Thiophene hydrodesulfurization over transition metal zeolites. *Surf. Technol.* **1980**, *10*, 379.

Burch, R.; Collins, A. Metal sulfide-support interactions. *J. Catal.* **1986**, *97*, 385.

Cid, R.; Villasenor, J.; Orellana, F.; Fierro, J. L. G.; Lopez Agudo, A. Surface and catalytic properties of alumina-, silica-, and NaY zeolite supported CoMo catalysts. *Appl. Catal.* **1985**, 18, 357.

Cid, R.; Fierro, J. L. G.; Lopez Agudo, A. Characterization and reactivity of sulfided NiNaY zeolite catalysts for thiophene conversion. *Zeolites* **1990**, *10*, 95.

Davidova, N.; Kovacheva, P.; Shopov, D. ESR study of zeolites containing transition metals and their hydrodesulfurization activity. *Zeolites* **1986**, *6*, 304.

Eijsbouts, S.; de Beer, V. H. J.; Prins, R. Periodic trends in the hydrodenitrogenation activity of carbon supported transition metal sulfide catalysts. *J. Catal.* **1988**, *109*, 217.

Eijsbouts, S.; de Beer, V. H. J.; Prins, R. Hydrodenitrogenation of quinoline over zeolite supported transition metal sulfides. *J. Catal.* **1991a**, *127*, 619.

Eijsbouts, S.; Sudhakar, C.; de Beer, V. H. J.; Prins, R. Hydrodenitrogenation of decahydroquinoline, cyclohexylamine and *o*-propylaniline over carbon-supported transition metal sulfide catalysts. *J. Catal.* **1991b**, *127*, 605.

Esener, A. A.; Maxwell, I. E. Improved hydrocracking performance by combined conventional hydrotreating and zeolite catalysts in stacked bed reactors, In *Advances in Hydrotreating Catalysts*; Ocelli, M. L., Anthony, R. G., Eds.; Elsevier: Amsterdam, 1989; p 263.

Haag, W. O.; Dessau, R. M. Duality of mechanism in acid catalyzed parafin cracking, In *Proc. Eighth Int. Congr. Catal.*, Berlin; Verlag Chemie: Weinheim, 1984; Part II, p 305.

Jacobs, P. A.; Martens, J. A. Introduction to acid catalysis with zeolites in hydrocarbon reactions. *Stud. Surf. Sci. Catal.* **1991**, *58*, 445.

Jacobs, P. A.; Uytterhoeven, J. B.; Steyns, M.; Froment, G.; Weitkamp, J. Hydroisomerization and hydrocracking I: comparison of the reactions of *n*-decane over USY and ZSM-5 zeolites containing platinum. In *Proc. Seventh Int. Conf. Zeolites*; Rees, L. V. C., Ed.; Heyden: London, 1980; p 607.

Kovacheva, P.; Davidova, N.; Novakova, J. Characterization of molybdenum and/or nickel containing zeolites, used as catalysts for hydrodesulfurization. *Zeolites* **1991**, *11*, 54.

Lacroix, M.; Boutarfa, N.; Guillard, C.; Vrinat, M.; Breysse, M. Catalytic properties in hydrotreating reactions of ruthenium sulfides on Y zeolites: Influence of the support acidity. *J. Catal.* **1989**, *120*, 473.

Langois, G. E.; Sullivan, R. F.; Egan, C. J. The effect of sulfiding a nickel on silica-alumina catalyst. *J. Phys. Chem.* **1966**, *70*, 3666.

Laniecki, M.; Zmierczack, W. Sulfided Ni-Mo-Y zeolites as catalysts for hydrogenation and hydrodesulfurization reactions. In *Zeolite chemistry and catalysis*; Jacobs, P. A., et al., Eds.; Elsevier: Amsterdam, 1991; p 331.

Ledoux, M. L.; Michaux, O.; Agostini, G.; Panissod, P. The influence of sulfide structures on the hydrodesulfurization activity of carbon supported catalysts. *J. Catal.* **1986**, *102*, 275.

Leglise, J.; Janin, A.; Lavalley, J. C.; Cornet, D. Nickel and molybdenum sulfides loaded into zeolites: activity for catalytic hydrogenation. *J. Catal.* **1988**, *114*, 388.

Leglise, J.; Chambellan, A.; Cornet, D. Hydroconversion of *n*-nonane catalyzed by PdHY zeolites. I: Influence of catalyst pretreatment. *Appl. Catal.* **1991a**, *69*, 15.

Leglise, J.; el Qotbi, M.; Goupil, J. M.; Cornet, D. Competitive reactions catalyzed by NiMo-containing zeolites. *Catal. Lett.* **1991b**, *10*, 103.

Lunsford, J. H.; Treybig, D. S. ESCA evidence for the occlusion of platinum particles in reduced PtY zeolites. *J. Catal.* **1981**, *68*, 192.

Mangnus, P. J. Characterization of hydrotreating catalysts with temperature programmed techniques. Ph.D. Thesis, University of Amsterdam, The Netherlands, 1991.

Martens, J. A.; Jacobs P. A.; Weitkamp, J. Attemps to rationalize the distribution of hydrocracked products. I: Qualitative desorption of the primary hydrocracking modes of long chain paraffins in open zeolites. *Appl. Catal.* **1986a**, *20*, 239.

Martens, J. A.; Jacobs, P. A.; Weitkamp, J. Attemps to rationalize the distribution of hydrocracked products. II: Relative rates of primary hydrocracking modes of long chain paraffins in open zeolites. *Appl. Catal.* **1986b**, *20*, 283.

Mirodatos, C.; Barthomeuf, D. Cracking of *n*-decane on zeolite catalysts: Enhancement of light hydrocarbon formation by the zeolite field gradient. *J. Catal.* **1988**, *114*, 121.

Pecoraro, T. A.; Chianelli, R. R. Hydrodesulfurization catalysis by transition metal sulfides. *J. Catal.* **1981**, *67*, 430.

Scheffer, B.; Mangnus, P. J.; Moulijn, J. A. A temperature-programmed sulfiding study of $NiOWO_3/Al_2O_3$ catalysts. *J. Catal.* **1990**, *121*, 18.

Schulz, H.; Weitkamp, J. Hydrocracking and hydroisomerization of *n*-dodecane. *Ind. Eng. Chem. Prod. Res. Dev.* **1972**, *11*, 46.

Sie, S. T. Acid catalyzed cracking of paraffinic hydrocarbons. 3. Evidence for the protonated cyclopropane mechanism from hydrocracking/hydroisomerization experiments. *Ind. Eng. Chem. Res.* **1993**, *32*, 403.

Sinfelt, J. H. Specificity in catalytic hydrogenolysis by metals. *Adv. Catal.* **1973**, *23*, 91.

Steijns, M.; Froment, G.; Jacobs, P. A.; Uytterhoeven, J. B.; Weitkamp, J. Hydroisomerization and hydrocracking. II: Product distributions from *n*-decane and *n*-dodecane. *Ind. Eng. Chem. Prod. Res. Dev.* **1981**, *20*, 654.

Vasquez, M. I.; Escardino, A.; Corma, A. Activity and selectivity of Ni-Mo/HYUS for hydroisomerization and hydrocracking of alkanes. *Ind. Eng. Chem. Res.* **1987**, *26*, 1495.

Vissers, J. P. R.; Groot, C. K.; van Oers, E. M.; de Beer, V. H. J.; Prins, R. Carbon supported transition metal sulfides. *Bull. Soc. Chim. Belg.* **1984**, *93*, 813.

Ward, J. W. Design and preparation of hydrocracking catalysts. *Stud. Surf. Sci. Catal.* **1983**, *16*, 587.

Ward, J. W. Hydrocracking processes and catalysts. *Fuel Proc. Technol.* **1993**, *35*, 55.

Weitkamp, J. The influence of the chain length in hydrocracking and hydroisomerization of n-alkenes. *ACS Symp. Ser.* **1975**, *20*, 1.

Weitkamp, J. Hydrocracken, cracken und isomerisieren von kohlenwasserstoffen. *Erdoel Kohle, Erdgas, Petrochem.* **1978**, *31*, 13.

Weitkamp, J. Isomerization of long chain *n*-alkanes on a Pt/CaY catalysts. *Ind. Eng. Chem. Prod. Res. Dev.* **1982**, *21*, 550.

Welters, W. J. J.; Vorbeck, G.; van Oers, E. M.; Zandbergen, H. W.; van de Ven, L.; de Haan, J. W.; de Beer, V. H. J.; van Santen, R. A. NaY supported molybdenum sulfide catalysts prepared via impregnation with amonium heptamolybdate. Submitted for publication to *J. Catal.* **1994a**.

Welters, W. J. J.; Vorbeck, G.; Zandbergen, H. W.; de Haan, J. W.; de Beer, V. H. J.; van Santen, R. A. HDS activity and characterization of zeolite supported nickel sulfide catalysts. *J. Catal.* **1994b** *150*, 155.

Yan, T. Y. Effect of metal on zeolite catalysts for extinction hydrocracking. *Ind. Eng. Chem. Res.* **1990**, *29*, 1995.

Received for review April 26, 1994
Revised manuscript received November 4, 1994
Accepted November 25, 1994[⊗]

IE940269P

[⊗] Abstract published in *Advance ACS Abstracts,* February 15, 1995.